# Formation of Photoresponsive Uniform Colloidal Spheres from an Amphiphilic Azobenzene-Containing Random Copolymer

**Yaobang Li, Yonghong Deng, Xiaolan Tong, and Xiaogong Wang***

*Department of Chemical Engineering, School of Material Science and Engineering, Tsinghua University, Beijing, P. R. China, 100084*

*Received October 20, 2005; Revised Manuscript Received November 26, 2005*

ABSTRACT: Photoresponsive uniform colloidal spheres were constructed from an amphiphilic azobenzene-containing random copolymer, poly{2-[4-(phenylazo)phenoxy]ethyl acrylate-*co*-acrylic acid} (PPAPE), and were characterized by using TEM, SEM, AFM, SLS, and DLS measurements. The photoisomerization of the azobenzene units was studied and used as a tool to probe the structure variation during the sphere formation process. The spheres were formed through gradual hydrophobic aggregation of the polymeric chains in THF−$H_2O$ dispersion media, which was induced by a steady increase in the water content. The polymeric chains started to aggregate and form the colloidal spheres at the critical water content (CWC). CWC was related with the initial concentration of the polymer in the THF solution and estimated to be 25% (vol %) when the initial concentration was 1.0 mg/mL. The colloids grew as the water content increased above the CWC. After the water content reached 40−50% (vol %), both the trans-to-cis photoisomerization rate and the isomerization degree at the photostationary state decreased significantly as the water content increased. It indicated that the isomerization was hindered by the polymeric chain collapse and entanglement occurring at this stage of the sphere growth process. Upon UV light irradiation, the photoinduced deaggregation behavior of the spheres was controlled by the water contents of the dispersion media. The understanding obtained from above observations can give some insight into the mechanism for the formation of the uniform colloidal spheres from polydispersed random copolymers and can be used to control the colloidal structures by adjusting the preparation conditions.

## 1. Introduction

Colloidal particles, which have at least one dimension within the nanometer to micrometer range, have been widely applied in many industrial products such as inks, paints, coatings, cosmetics and photographic films among others.[1] Recently, study on polymer-based colloidal particles has aroused broad interests in new areas such as drug-delivery, biodiagnostics, and combinatorial synthesis.[2−6] Monodispersed colloidal spheres have been widely used to construct two-dimensional (2D) and three-dimensional (3D) ordered colloidal arrays, which can potentially be used in sensors, filters, optical switches, photovoltaic devices, soft-lithographic process and photonic band gap (PBG) materials among others.[7−10] Uniform colloidal spheres composed of the major type of functional polymers can further expand the functionalities of those colloid-based materials.[7,11−13]

Polymers containing aromatic azo chromophores (azo polymer for short) have been extensively investigated in recent years.[14−21] Due to the trans−cis photoisomerization of azobenzene units, azo polymers can show various photoinduced responses in their structures and properties, such as phase transition, photoinduced chromophore orientation, surface-relief-gratings (SRGs), light-driven contraction and bending.[15,16,21] Azo polymers are promising for applications in photoswitching, optical data-storage, sensors, light-driven reactors, and artificial muscles.[17−21] Incorporating azo polymers into colloidal particles can further enhance those interesting properties and lead to new applications in various photodriven devices.

Emulsion polymerizations based on free-radical chain reactions have been widely applied to prepare polymer-based colloidal spheres with narrow size distribution.[22] However, due to the inhibition of azo groups to the free-radical chain reaction, emulsion polymerization can hardly be used to prepare polymers that contain a large amount of azo chromophores. Micellar spheres can be prepared from block or graft copolymers through self-assembly of the polymeric chains by using a suitable selective solvent.[23,24] Amphiphilic block copolymers can form uniform micellar spheres with a hydrophobic core and a hydrophilic corona in aqueous media or form reverse micelles in organic solvents. Depending on the relative size of the core and corona, two types of the aggregates, termed as "starlike" micelles and "crew-cut" micelles, can be prepared.[23, 24(e)] In general, uniform micelles can only be obtained from block copolymers that are monodispersed in both the molecular weight and block length. Those well-defined copolymers are prepared by some rather sophisticated polymerization methods, such as the anionic living polymerization and atomic transfer radical polymerization (ATRP). Recently, micellar aggregates have been prepared from amphiphilic diblock azo copolymers synthesized by ATRP.[25] The aggregates show interesting photoinduced deaggregation behavior caused by the photoisomerization of the azo chromophores.

Recently, we have reported that through gradual hydrophobic aggregation, uniform colloidal spheres can be constructed from amphiphilic azo polymers possessing a relatively broad distribution in the molecular weight or the degree of functionalization (i.e., hydrophobicity).[26,27] Those azo polymers can be prepared by ordinary radical polymerization or polycondensation. The colloidal spheres show some interesting properties such as photoinduced shape deformation,[26] and photoinduced dichroism.[27] However, some important issues concerning the forming mechanism and inner structure of those colloidal spheres have not yet been fully understood.

In this work, an amphiphilic azobenzene-containing random copolymer, which has polydispersity in both the molecular weight and the degree of functionalization, was used to construct

* Corresponding author: wxg-dce@mail.tsinghua.edu.cn.

10.1021/ma052272y CCC: $33.50 © 2006 American Chemical Society
Published on Web 01/07/2006

colloidal spheres through the gradual hydrophobic aggregation scheme. Instead of the pseudo-stilbene-type azo chromophores used in our previous work,[26,27] the polymer was designed to contain the azobenzene-type chromophores, which possess a relatively stable cis-form and the photoisomerization can be monitored by UV−vis spectroscopy.[28] The forming process and morphology of the colloidal spheres were characterized by the transmission electron microscopy (TEM), scanning electron microscopy (SEM), atom force microscopy (AFM), static light scattering (SLS) and dynamic light scattering (DLS). The photoisomerization behavior of the azobenzene units was used as a probe to detect the local structure in the colloidal spheres. Results indicate that the polymeric chains start to aggregate at the critical water content (CWC) and collapse gradually during the sphere growth process as the water content in the dispersion media increases. Upon UV light irradiation, the photoinduced deaggregation behavior of the spheres depends on the water contents of the dispersion media.

## 2. Experimental Section

**Materials.** Analytical pure tetrahydrofuran (THF) from commercial source was refluxed with cuprous chloride and distilled for dehydration before use. Deionized water (resistivity > 18 MΩ) was obtained from a Millipore water purification system and used for the experiments described below. Poly{2-[4-(phenylazo)-phenoxy]ethyl acrylate-*co*-acrylic acid} (PPAPE) was prepared by the Schotten−Baumann reaction between poly(acryloyl chloride) and 2-[4-(phenylazo)phenoxy]ethanol, and the unreacted acyl chloride groups were then hydrolyzed to obtain the carboxyl groups. The preparation and characterization details can be seen in our previous paper.[29] The PPAPE sample used in this study had the degree of functionalization (DF) of 49.9%, defined as the percentage of the structure units bearing azo chromophores among the total units. The molecular weight and its distributions of PPAPE were estimated by carrying out the gel permeation chromatography (GPC) measurement on a poly(methyl acrylate) sample that was prepared by the reaction between the same batch of poly(acryloyl chloride) and excessive methanol. The GPC instrument utilized a Waters model 515 pump and a model 2410 differential refractometer with three Styragel columns, HT2, HT3, and HT4, connected in a serial fashion. THF was used as the eluent at a flow rate of 1.0 mL/min. Polystyrene standards with dispersity of 1.08−1.12 obtained from Waters were employed to calibrate the instrument. The number-average molecular weight ($M_n$) and the weight-average molecular weight ($M_w$) of PPAPE estimated by this method were $6.53 \times 10^4$ and $1.24 \times 10^5$, respectively.

**Preparation of Colloidal Spheres.** Suitable amounts of PPAPE samples were dissolved in THF to obtain solutions with different initial concentrations (range from 0.05 to 1.0 mg/mL). The solutions were under stirring for 1 day and then put aside for at least 72 h. To obtain suspensions of the colloidal spheres in THF−$H_2O$ media with different water contents, the required amounts of water were added into the THF solutions at a rate of 5−6 drops per minute with durative stirring. For preparation of the stable colloidal suspensions, water was added into the THF solutions in the same manner until the water content reached 50% (vol %). After that, an excess of water was added into the suspensions to "quench" the structures formed. The suspensions were dialyzed against water for 3 days to remove THF before further measurements.

**Transmission Electron Microscopy (TEM).** TEM images of the colloidal spheres were obtained by using a JEOL-JEM-1200EX microscope with an accelerating voltage of 120 kV. The TEM samples were prepared by dropping diluted sphere suspensions onto the copper grids coated with a thin polymer film and then dried in a 30 °C vacuum oven for 24 h. No staining treatment was performed for the measurement.

**Atom Force Microscopy (AFM) and Scanning Electron Microscopy (SEM).** Samples for the measurements were prepared by casting the suspensions on silicon wafers and dried in a constant humidity oven at 30 °C for 24 h. AFM images were obtained by using a Scanning Probe microscope (Nanoscope IIIa) in the tapping mode. SEM images were obtained with a field emission microscope (JEOL-6301F), which was operated with an accelerating voltage of 5 kV. All the samples prepared for SEM studies were coated with thin layers of gold (~15 nm in thickness) before the measurements.

**Light Scattering Measurement.** Light scattering measurements were performed by using a Wyatt DAWN-EOS multiangle laser photometer equipped with a He−Ne laser (632.8 nm) and a Wyatt QELS equipment. A field-flow fractional (FFF) system was used for the separation of the colloidal spheres with different sizes before the measurements. The "field" for cross-flow FFF was provided by the water "cross-flow" which pushed particles against the accumulation wall (membrane). Larger particles had smaller diffusion coefficients and were pushed more effectively. The parabolic channel flow profile then separated the particles by size and the smallest ones were eluted out first. The experimental light scattering data of each component were analyzed by the Debye plot method. The refractive index increment value, d$n$/d$C$, was measured to be 0.2246 by an OTSUKA Rm-102 differential refractometer.

The size and size distribution of the colloidal spheres were also measured with a Marvern Zetasizer 3000 dynamic light scattering instrument equipped with a multi-$\tau$ digital time correlation and a 632 nm solid-state laser light source. The scattering angle used for the measurement was 90° and the sample temperature was controlled to be 25 °C.

**Photoisomerization Study.** The photoisomerization of the azo chromophores was induced by irradiating UV light, which was from a high-intensity 365 nm UV lamp equipped with 12.7 cm diameter filter (Cole-Parmer L-97600-05 long wave UV lamp, L-09819-23 filter). The intensity of the lamp was 7000 mW/cm$^2$ at a distance of 38 cm and 21000 mW/cm$^2$ at a distance of 5 cm. The samples were placed at ca. 15 cm away from the lamp. The surrounding temperature of the samples was controlled to be about 30 °C by a cold plate. The UV−vis spectra of the samples were measured over different irradiation time intervals by using an Agilent 8453 UV−vis spectrophotometer. For measuring the thermal cis-to-trans isomerization, the samples were kept in a dark oven with constant temperature (30 ± 1 °C), and the UV−vis spectra were recorded over different time intervals.

To study the effect of the water content on photoresponsive behavior of the colloidal spheres, the colloidal sphere suspensions with different water contents were prepared by the method mentioned above. Then each suspension was divided into two parts, one part was irradiated with the UV light, and the UV−vis spectra were recorded over different time intervals until the photostationary state was reached, and the other part was used as a control without the light irradiation. After that, an excessive amount of water was added into the suspensions to quench the structures. The TEM samples were prepared and characterized by the method described above.

## 3. Results and Discussion

The chemical structure and synthetic scheme of the amphiphilic azo copolymer (PPAPE) used in this study are given as

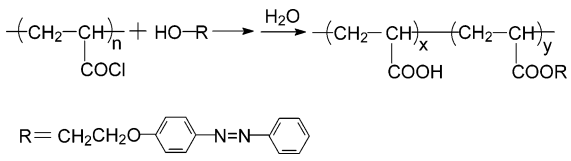


PPAPE is a random copolymer composed of hydrophilic acrylic acid units and hydrophobic azobenzene-containing acrylate units. Because of the synthetic method, the hydrophobic units are randomly distributed along the polymeric chain. The polymer

CDV

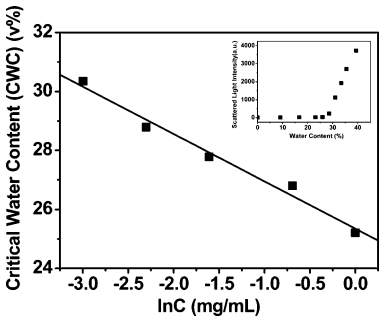


**Figure 1.** Plot of the critical water content (CWC) vs ln(*C*), where *C* is the initial PPAPE concentrations in THF solutions. Inset: scattering light intensity as a function of the water content (vol %) in the THF−$H_2O$ dispersion media, the initial concentration of PPAPE in THF is 1.0 mg/mL.

possesses polydispersity both in the molecular weight and in the loading density of the hydrophobic units. The degree of functionalization (DF) is defined as the percentage amount of azobenzene units among total units. DF of the sample used for this study was measured to be 49.9%, which should be understood as a statistically averaged value. The $M_n$ and $M_w$ of PPAPE were $6.53 \times 10^4$ and $1.24 \times 10^5$, respectively.

**3.1. Preparation of the Colloidal Spheres.** Colloidal spheres were prepared by a method similar to those used by Eisenberg et al. for preparing "crew-cut" micelles from amphiphilic block copolymers.[24a,30,31] In the current work, water was gradually added into homogeneous solutions of PPAPE in THF. When the water content reached a critical value, the scattered light intensity was observed to increase suddenly, which indicated that the azo polymer chains started to aggregate in the solutions. Similar to the previous work,[32] the water content at this point is defined as the critical water content (CWC).

The CWC values were obtained by measuring the variation curves of the scattered light intensity of the samples with the water contents. The inset of Figure 1 shows a typical plot of the scattered light intensity vs the water content. When the water content is low, the scattered light intensity is almost zero and remains unchanged as the water content increases. When the water content reaches CWC, ca. 25% (vol %) in this case, the scattered light intensity increases sharply. For amphiphilic block copolymers, CWC depends on both the polymer concentration and the molecular weight of the polymers.[32] The higher the polymer concentration and the molecular weight, the lower the CWC. A similar tendency can be seen from the plot of CWC as a function of the initial concentration of PPAPE in THF (Figure 1). When the initial concentration increases from 0.05 mg/mL to 1.0 mg/mL, CWC decreases from 30.4% (vol %) to 25.2% (vol %). A linear relationship is found between CWC and the logarithm of the polymer concentration. The initial concentration of PPAPE in THF can be used as a parameter to adjust the size of the colloidal spheres. The size of the colloidal spheres increases as the initial concentration increases.[27] By changing the initial concentration in the range mentioned above, the average size of the colloids can be adjusted from 80 to 180 nm.

At the final stage of the sphere preparation process, an excess of water was added into the suspensions to "quench" the structures formed. The suspensions were dialyzed against water to remove THF and the stable water suspensions of the spheres were obtained.

**3.2. Characterization of the Colloidal Spheres.** Figure 2 shows a typical TEM image of the colloidal spheres, which were formed from a solution with the initial concentration of 1.0 mg/mL. The average size of the spheres was estimated to be 180 nm, obtained based on the statistics of 100 contiguous spheres in the TEM images. Colloidal spheres with a smaller average size can be obtained by decreasing the initial concentration of PPAPE in the THF solution. A SEM image of the spheres is given in Figure 3. The size estimated from the SEM image is consistent with the TEM observation. Both TEM and SEM observations indicate that the spherical colloids are rather uniform in their sizes. Parts a and b of Figure 4 give typical AFM images of the spheres casting from the suspension on a clean wafer surface. The section analysis of the surface is shown in Figure 4c, which is obtained from the top view image given in Figure 4b. It can be seen that the heights from the top of the spheres to the substrate are about 150 nm, while the horizontal diameters of the spheres are about 200 nm. It indicates that the colloidal spheres are somewhat soft and dent to the substrate under the tipping action.

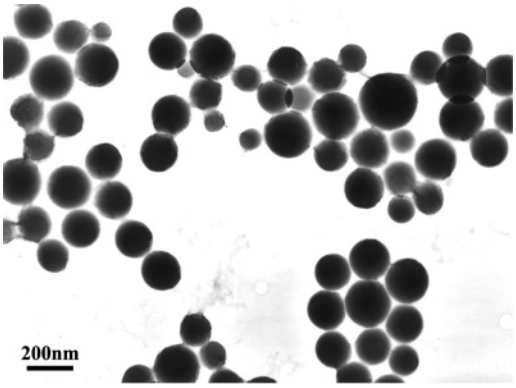


**Figure 2.** Typical TEM image of the colloidal spheres obtained from the water suspension, which was prepared by dropping water into the THF solution until 50% (vol %), then "quenched" with excess of water and dialyzed against water for 3 days. The initial concentration of PPAPE in THF is 1.0 mg/mL.

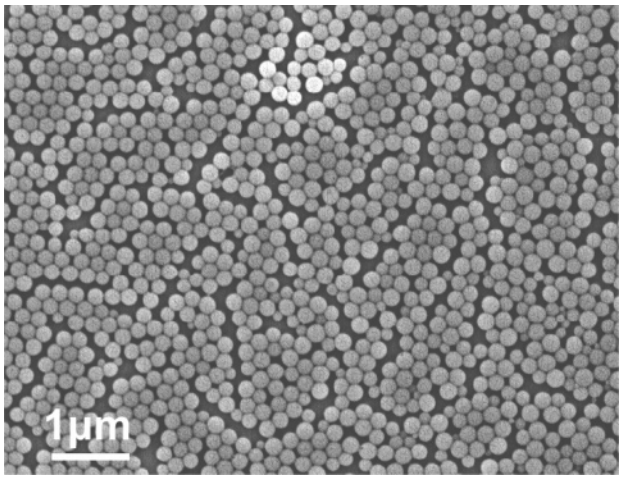


**Figure 3.** Typical SEM image of the colloidal spheres obtained from the water suspension, which was prepared by dropping water into the THF solution until 50% (vol %), then "quenched" with excess of water and dialyzed against water for 3 days. The initial concentration of PPAPE in THF is 1.0 mg/mL.

Light scattering was used to further characterize the size, size distribution and aggregation number of the colloidal spheres. The dynamic light scattering (DLS) shows a monomodal distribution for the sizes of the colloidal spheres. Figure 5a gives the size distribution curve obtained from DLS measurement, which shows a hydrodynamic radius ($R_h$) of 93 nm. The radius of gyration ($R_g$) of the sample was estimated to be 72 nm by SLS, obtained from the initial slope of the Debye Plot (Figure

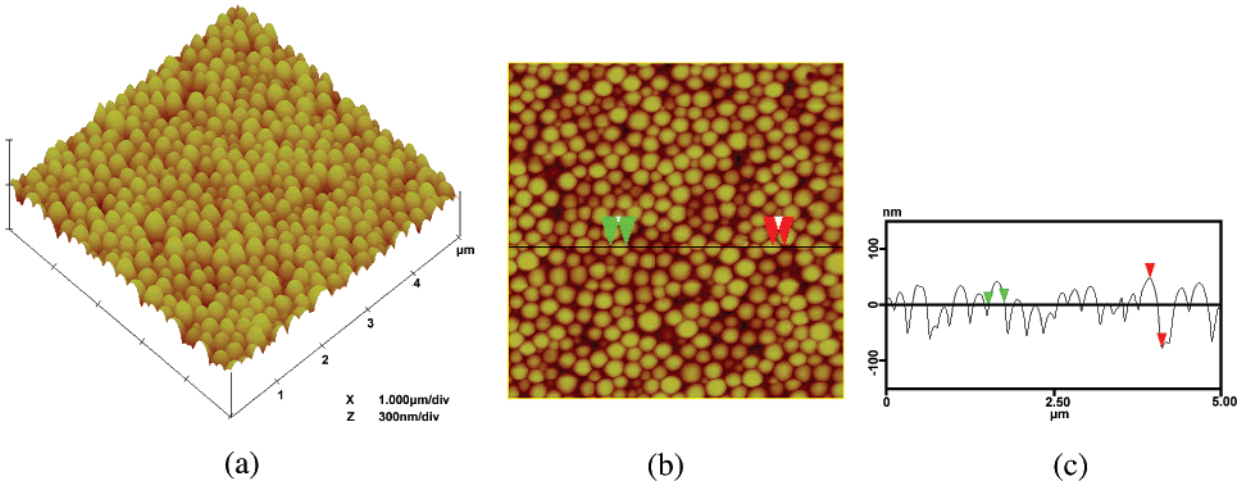


**Figure 4.** AFM images of the colloidal spheres obtained from the water suspension, which was prepared by dropping water into the THF solution until 50% (vol %), then "quenched" with excess of water and dialyzed against water for 3 days. The initial concentration of PPAPE in THF is 1.0 mg/mL. Key: (a) surface plot, (b) top view, and (c) section analysis.

**Table 1. DLS and LLS Experimental Results of the Colloidal Spheres**[a]

| colloidal spheres | $R_h$ (nm) | $\mu_2/\Gamma^2$ | $R_g$ (nm) | $R_g/R_h$ | $MW_{sphere}$ (g/mol) | $N_{agg}$[b] | $\rho$[c] (g/cm$^3$) |
|---|---|---|---|---|---|---|---|
| | $93 \pm 4.0$ | 0.030 | $72.1 \pm 0.7$ | 0.775 | $(1.55 \pm 0.05) \times 10^8$ | 1249 | 0.076 |

[a] Here $\mu_2/\Gamma^2$ is the polydispersity index of the spheres in the water suspension measured by the dynamic light scattering. [b] $N_{agg} = MW_{sphere}/MW_{polymer}$. [c] $\rho = MW_{sphere}/(N_A 4\pi\langle R_h\rangle^3/3)$.

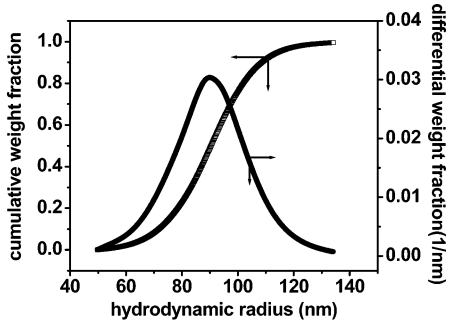


(a)

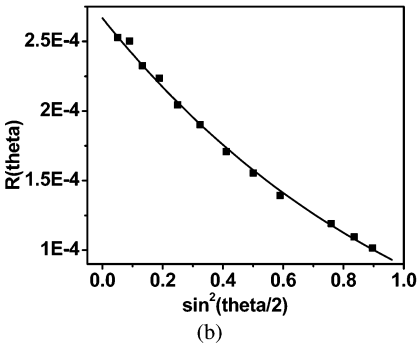


(b)

**Figure 5.** (a) Cumulative size distribution and differential weight fraction of the colloidal spheres from the DLS. (b) Debye plot of the static light scattering data. The spheres were prepared from a THF solution with the initial polymer concentration of 1.0 mg/mL.

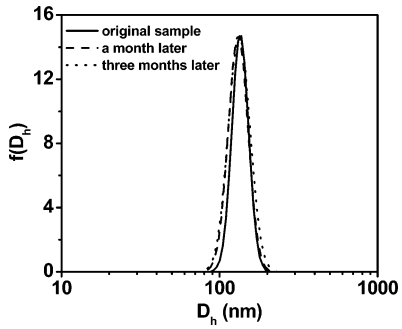


**Figure 6.** Hydrodynamic diameter distributions of the colloidal spheres in water suspensions, measured immediately after preparation, a month later, and 3 months later. The suspensions were prepared by dropping water into the THF solutions until 50% (vol %), then "quenched" with excess of water and dialyzed against water for 3 days. The average hydrodynamic diameter ($D_h$) of the spheres is about 140 nm. The initial concentrations of PPAPE in THF are 0.5 mg/mL.

5b). The results obtained from the light scattering measurement are summarized in Table 1. The $R_g/R_h$ value can be used to characterize the shape of aggregates. For spheres with uniform density, $R_g/R_h$ is equal to 0.775.[33] $R_g/R_h$ estimated in the current work is around 0.775, which means that the PPAPE colloids are spherical and possess uniform density. The average aggregate number in each sphere is estimated to be 1249, calculated from $N_{agg} = MW_{sphere}/MW_{polymer}$, where $MW_{sphere}$ and $MW_{polymer}$ are the weight-average mass of the colloidal spheres and the weight-average molecular weight of the polymer.[24b] The apparent density of the spheres is calculated to be 0.076 g/cm$^3$ by applying the following equation[34]

$$\rho = MW_{sphere}/(N_A\, 4\pi\, \langle R_h\rangle^3/3) \qquad (1)$$

where $N_A$ is Avogadro's constant. The apparent density of the azo polymer spheres is higher than the "crew-cut" micelles formed from block and graft copolymers.[24b,34]

The size and its distribution of the spheres were measured after different storage time to test the stability of the colloidal spheres in the water suspensions. No obvious variation was observed from the DLS measurement after storage at room temperature for three months (Figure 6). The result was also confirmed by the TEM observation. The colloidal spheres can be precipitated from the suspensions by evaporation of the dispersing media ($H_2O$) and can be dispersed again by adding $H_2O$. It is believed that the colloidal spheres are stabilized by the repulsive electrostatic interaction of the surface charges.

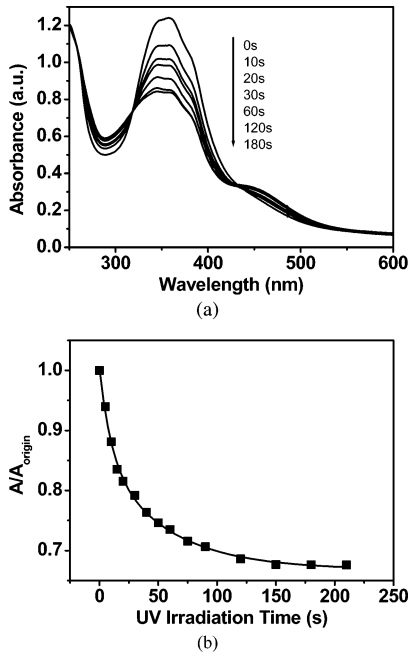


**Figure 7.** (a) Variation of the UV−vis spectra of the spheres in the water suspension induced by the UV light irradiation. (b) Relative absorbance ($A/A_{origin}$) varying with the irradiation time and the fitting curve. The suspension was prepared by dropping water into the THF solution until 50% (vol %) and then "quenched" with excess water and dialyzed against water for 3 days. The initial concentration of PPAPE in THF is 0.5 mg/mL.

**3.3. Photoisomerization Study.** As the photoisomerization of azobenzene units is sensitive to the local environments surrounding the units, information about the local structure and its variation can be obtained by measuring the isomerization rate and the isomerization degree at the photostationary state.[14,35] In this study, the suspensions of the colloidal spheres were irradiated with 365 nm UV light for different time intervals and the UV−vis spectra of the samples were recorded until the photostationary states were reached. A series of UV−vis spectra of the suspension varying with the irradiation time is given in Figure 7a. Upon the UV light irradiation, the absorbance of the $\pi-\pi^*$ transition band at 360 nm decreases and the absorbance of the $n-\pi^*$ transition band at 450 nm increases gradually. The spectral variations evidence the trans-to-cis isomerization of the azobenzene-type chromophores.[28,35−38] When the sample was kept in the dark, the spectra gradually recovered to the original curve, which indicated that the azo chromophores undergo a slow thermal isomerization back from the cis form to the trans form. The relative absorbance $A(t)$ ($= A/A_{origin}$), where $A_{origin}$ and $A$ are the absorbance at 360 nm before the light irradiation and after the irradiation for different time, can be best fitted by the first-order exponential decay function,

$$A(t) = A_0 + A_1 \exp(-t/T_1) \qquad (2)$$

in which $T_1$ is the characteristic time of the decay process. Both data and fitting curve are shown in Figure 7b and the parameters obtained from the best fit are given in Table 2.

For comparison, the photoisomerization of PPAPE in a THF solution (0.04 mg/mL) was also detected under the same UV light irradiation condition. Its kinetic curve can also be best fitted by the first-order exponential decay function. The parameters obtained from the fit are also given in Table 2. It shows that the trans-to-cis isomerization rate is much slower for the colloidal spheres ($T_1 = 27.6$) than that for the THF solution ($T_1 = 2.62$). Compared with our previous results,[29] it can be seen that the isomerization rate of azo chromophores in colloidal spheres is also much slower than those observed for PPAPE molecules that have low DF (15.0%) and are homogeneously dissolved in water solutions. The slow isomerization rate is a result of the polymeric chain collapse and entanglement occurring in the sphere formation process, which will be discussed in the following part.

**Table 2. Parameters of the Photoisomerization Kinetics Obtained from the Curve Fitting for the Water Suspension of the Spheres and the THF Solution of PPAPE[a]**

| samples | $A_0$ | $A_1$ | $T_1$ (s) | $\chi^2$ |
|---|---|---|---|---|
| THF solution | 0.10 | 0.89 | 2.62 | $1.4 \times 10^{-4}$ |
| water suspension | 0.68 | 0.31 | 27.6 | $1.2 \times 10^{-3}$ |

[a] Here $\chi^2$ is the mean squared error of the fitting.

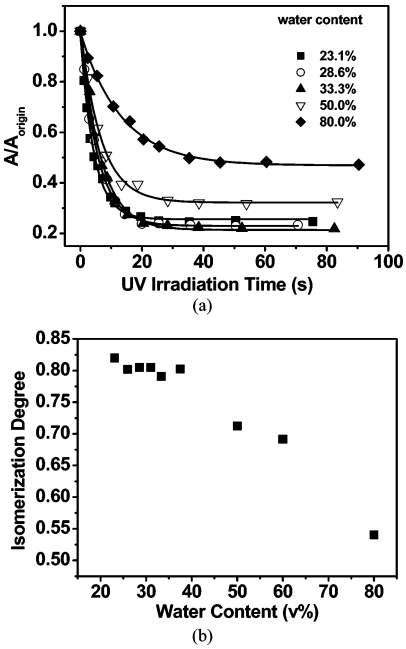


**Figure 8.** (a) Plot of the relative absorbance ($A/A_{origin}$) of the aggregates vs the irradiation time for suspensions with different water contents. (b) Relationship between the isomerization degree at the photostationary state and the water content. The spheres were prepared from a THF solution with the initial polymer concentration of 0.5 mg/mL.

**3.4. Effect of the Water Content on the Photoisomerization.** To understand the structure variation in the sphere formation process, a series of suspensions with the different water contents were prepared. The photoisomerization of azobenzene units in the suspensions was studied by UV−vis spectroscopy. Figure 8a shows the relative absorbance ($A/A_{origin}$) of the suspensions as a function of the UV light irradiation time. The suspensions have an initial concentration of 0.5 mg/mL and different water contents. When the water content is in a range from 23.1% to 33.3% (vol %), the trans-to-cis photoisomerization kinetics is similar for the suspensions. As CWC is 26.8% (vol %) obtained from light scatting measurement, the observation indicates that the isomerization rate does not change significantly just above CWC. When the water content further increases to 40−50% (vol %), the photoisomerization rate starts to decrease obviously. When the water content is even higher (80%, vol %), the isomerization rate decreases drastically, but it is still faster than that of the spheres obtained from the "quenching" and dialysis procedure (Figure 7b). The relative absorbance ($A/A_{origin}$) of the samples as a function of the irradiation time can be best fitted by the first-order exponential decay function. The parameters obtained from the fit are given

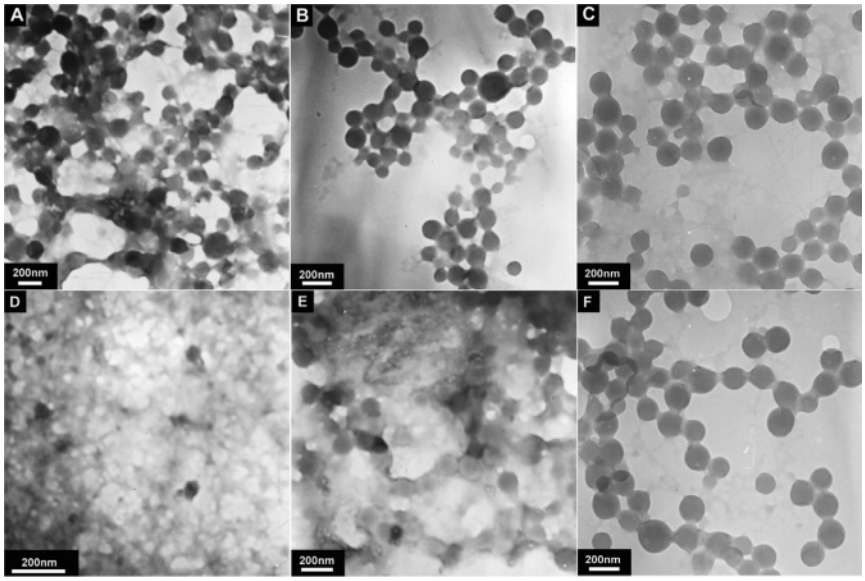


**Figure 9.** TEM images of the samples obtained from the suspensions before the UV light irradiation (A−C) and after the UV light irradiation for 10 min (D−F). Water content (vol %): (A and D) 37.5%; (B and E) 50%; (C and F) 80%. The spheres were prepared from a THF solution with the initial concentration of 0.5 mg/mL.

**Table 3. Parameters of the Photoisomerization Kinetics Obtained from the Curve Fitting for the Suspensions with Different Water Contents**

| samples (% water content) | $A_0$ | $A_1$ | $T_1$ (s) | $\chi^2$ |
|---|---|---|---|---|
| 23.1 | 0.21 | 0.79 | 4.31 | $3.7 \times 10^{-3}$ |
| 28.6 | 0.23 | 0.76 | 5.57 | $3.5 \times 10^{-3}$ |
| 33.3 | 0.25 | 0.72 | 6.39 | $5.2 \times 10^{-3}$ |
| 50.0 | 0.32 | 0.68 | 8.41 | $2.8 \times 10^{-3}$ |
| 80.0 | 0.46 | 0.52 | 13.9 | $4.4 \times 10^{-3}$ |

in Table 3. As the water content increases, $T_1$ gradually increases and approaches the value of the colloidal spheres in the water suspension, which can be seen from the data given in Table 2.

The trans-to-cis isomerization degree at the photostationary state can also be used to probe the effect of water content on the colloid structure variation. The isomerization degree at the photostationary state is estimated from[39]

$$\text{isomerization degree} = 1.05 \times (1 - A_s/A_{\text{origin}}) \qquad (3)$$

where $A_s$ is the 360 nm absorbance measured at the photostationary state. The result plotted vs the water content is given in Figure 8b. When the water content is in range from 25% to 37.5% (vol %), the isomerization degree is high (about 80%) and almost keeps constant with the water content increase. When the water content increases further, the isomerization degree starts to decrease. When the water content increases from 37.5% to 80% (vol %), the isomerization degree decreases from 80% to ca. 55%. For the spheres in the water suspension, obtained by quenching with an excessive amount of water and dialysis, the isomerization degree even decreases to 33%.

To study the morphology change upon the UV light irradiation, a series of suspensions with different water contents were irradiated with the UV light for 10 min. The formed structures were "quenched" with an excessive amount of water and collected for TEM observations. Figure 9 gives some typical TEM images of the samples together with those obtained from the same suspensions before the UV light irradiation. As being expected, when the water content is below CWC (26.8%, vol %), no colloidal spheres can be seen both before and after the light irradiation. When the water content is above CWC, colloidal spheres can be seen for all the samples before the light irradiation (Figure 9A-C). When the water content is 37.5% (vol %), the colloidal spheres can be disrupted by the light irradiation (Figure 9D). When water content is higher (50%, vol %), the colloidal spheres can be partially disaggregated by the light irradiation (Figure 9E). When the water content further increases (80%, vol %), no observable morphology variation can be seen from the TEM images after the UV light irradiation (Figure 9F). For the colloidal spheres obtained from the "quenching" and dialysis procedure, no morphology change was observed by the TEM observation after the UV light irradiation for 10 min.

The above study can give us a consistent picture about the effect of the water content on the aggregation structures and their photoresponsive behavior. When the water content is low (such as lower than 37.5%, vol %), the structures formed in the suspensions are loose and can be disrupted by the UV light irradiation as a result of the volume expansion and hydrophilicity increase caused by the trans-to-cis isomerization. As a result, the observed photoisomerization rate and isomerization degree are rather similar to those observed for the "isolated" polymer chains in the THF solution. When the water content increases to 40−50% (vol %), the polymer chains start to collapse and the photoisomerization is gradually hindered by the surroundings in the aggregates. When the water content in the dispersion media is high (such as 80%, vol %), the colloidal structures are "frozen" through the polymeric chain collapse and entanglement, and the trans-to-cis photoisomerization can no longer cause the deaggregation. As a consequence, only those azobenzene-units with enough free volume in the colloidal spheres can undergo the photoisomerization. Therefore, the observed photoisomerization rates and saturated isomerization degrees are low.

**3.5. Colloidal Sphere Formation Mechanism.** The aggregation of block and graft copolymers induced by the selective solvents is an enthalpy-driven process.[40] For amphiphilic diblock copolymers, it has been pointed out that the micellization of the copolymers occurs through phase separation caused by the hydrophobic interaction.[32] When the precipitant ($H_2O$) is added into THF solutions of the block copolymers, the solubility of the solvent to the hydrophobic blocks decreases and the Flory−Huggins interaction parameter ($\chi$) increases as the water content increases. The critical $\chi$ value, at which the micelles start to

CDV

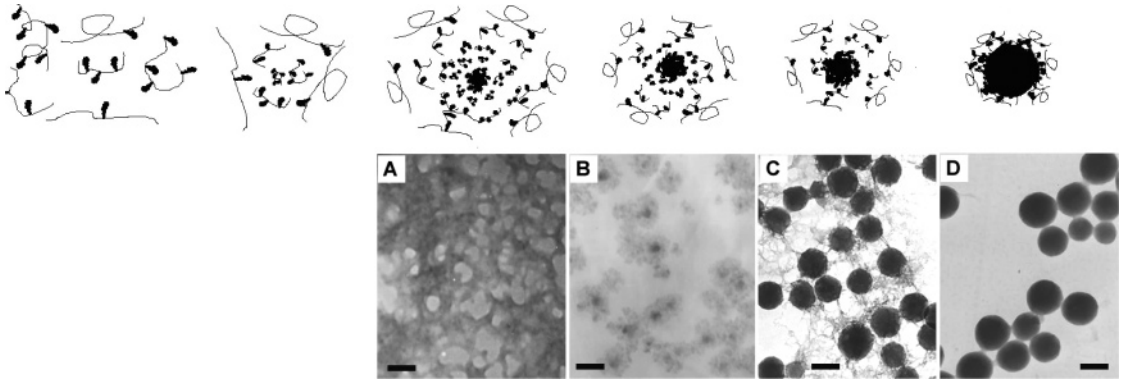


**Figure 10.** Schematic representation of the sphere formation process and the TEM images of the samples obtained from the suspensions with different water contents. Water content (vol %): (A) 20%, (B) 30%, (C) 40%, and (D) 50%. The scale bars in the figures are 100 nm.

form, decreases with the increase of the hydrophobic block length.[32]

In the current case, PPAPE possesses the polydispersity in both the molecular weight and the degree of functionalization (hydrophobicity). It is believed that the colloidal spheres form through a self-assembling process. When the water content is lower than CWC, the polymeric chains are soluble in the mixed solvent. When the water content reaches CWC, only a fraction of the polymer chains meets the phase separation condition because of the polydispersity. Those most hydrophobic chains or segments start to aggregate and form the cores of the colloidal spheres. As the water content further increases, more and more polymer chains meet the phase separation condition and transfer from the solution into the aggregates. Those polymer molecules gradually assemble on the cores, which is the colloidal sphere growth process. This growth process has been evidenced by the colloidal size increase with the water content increase, observed for a similar polymer in our previous work.[27] The above photoisomerization study indicates that the polymer chains collapse gradually and the colloidal structures are "frozen" in the process. In this nucleation and gradual growth process, polymeric chains organize themselves from cores to the shells in the hydrophobicity decrease order. The forming process is schematically represented in Figure 10. TEM images of the spheres obtained at the different forming stages are given in the same figure, which show the nucleation and gradual growth process. Because of this self-assembling process, the colloidal spheres have cores formed from the most hydrophobic chains and coronas composed of the most hydrophiphilic chains. Those structural characteristics are consistent with the above experimental results, such as the variation of the photoresponsive behavior and the high stability of colloidal spheres in the water suspensions.

## Summary

Photoresponsive uniform colloidal spheres of PPAPE were obtained through the gradual hydrophobic aggregation of the polymeric chains in THF−$H_2O$ dispersion media, induced by the steady increase of the water content. When the water content reached CWC, the polymeric chains started to aggregate and form the colloidal spheres. When the water content reached 40−50% (vol %), the polymeric chains collapsed gradually as the water content increased further, which was indicated by the decrease of both the trans-to-cis photoisomerization rate and the isomerization degree at the photostationary state. After the UV light irradiation, the colloids forming in the dispersion media containing a different amount of water showed different photoinduced deaggregation behavior.

**Acknowledgment.** Financial support from the NSFC under Projects 20374033 and 50533040 is gratefully acknowledged. The assistant of Dr. Michelle H. Chen is gratefully acknowledged for the SLS and some DLS measurements carried out in Wyatt research center, Santa Barbara, CA.

## References and Notes

(1) Hiemenz, P. C. *Principles of colloid and Surface Chemistry*, 2nd ed.; Marcel Dekker Inc.: New York, 1986.
(2) Chaibundit, C.; Ricardo, N. M. P. S.; Crothers, M.; Booth, C. *Langmuir* **2002**, *18*, 4277.
(3) Jeong, B.; Bae, Y. H.; Lee, D. S.; Kim, S. W. *Nature (London)* **1997**, *388*, 860.
(4) Moffitt, M.; Eisenberg, A. *Macromolecules* **1997**, *30*, 4363.
(5) Krämer, E.; Förster, S.; Göltner, C.; Antonietti, M. *Langmuir* **1998**, *14*, 2027.
(6) Lopes, W. A.; Jaeger, H. M. *Nature (London)* **2001**, *414*, 735.
(7) Xia, Y.; Gates, B.; Yin, Y.; Lu, Y. *Adv. Mater.* **2000**, *12*, 693.
(8) Ozin, G. A.; Yang, S. M. *Adv. Funct. Mater.* **2001**, *11*, 95.
(9) See, for example: (a) Jiang, P.; Bertone, J. F.; Hwang, K. S.; Colvin, V. L. *Chem. Mater.* **1999**, *11*, 2132. (b) Norri, D. J.; Arlinghaus, E. G.; Meng, L. L.; Heiny, R.; Scriven, L. E. *Adv. Mater.* **2004**, *16*, 1393. (c) Gu, Z. Z.; Fujishima, A.; Sato, O. *Chem. Mater.* **2002**, *14*, 760.
(10) Schroden, R. C.; Al-Daous, M.; Blanford, C. F.; Stein, A. *Chem. Mater.* **2002**, *14*, 3305.
(11) Tian, Z. Y.; Huang, W. T.; Xiao, D. B.; Wang, S. Q.; Wu, Y. S.; Gong, Q. H.; Yang, W. S.; Yao, J. N. *Chem. Phys. Lett.* **2004**, *391*, 283.
(12) Helseth, L. E.; Wen, H. Z.; Hansen, R. W.; Johansen, T. H.; Heining, P.; Fisher, T. M. *Langmuir* **2004**, *20*, 7323.
(13) Helseth, L. E.; Fisher, T. M. *Optics Express* **2004**, *12*, 3428.
(14) Kumar, G. S. *Azo Functional Polymers: Functional Group Approach in Macromolecular Design*, Technomic Publishing Company Inc.: Lancaster, PA, and Basel, Switzerland, 1993.
(15) Delaire, J. A.; Nakatani, K. *Chem. Rev.* **2000**, *100*, 1817.
(16) Natansohn, A.; Rochon, P. *Chem. Rev.* **2002**, *102*, 4139.
(17) Nikolova, L.; Todorov, T.; Ivanov, M.; Andruzzi, F.; Hvilsted, S.; Ramanujam, P. S. *Opt. Mater.* **1997**, *8*, 255.
(18) Xie, S.; Natansohn, A.; Rochon, P. *Chem. Mater.* **1993**, *5*, 403.
(19) Lee, S.-H.; Kumar, J.; Tripathy, S. K. *Langmuir* **2000**, *16*, 10482.
(20) Ichimura, K.; Oh, S. K.; Nakagawa, M. *Science* **2000**, *288*, 1624.
(21) (a) Li, M. H.; Keller, P.; Li, B.; Wang, X. G.; Brunet, M. *Adv. Mater.* **2003**, *15*, 569. (b) Yu, Y. L.; Nakano, M.; Ikeda, T. *Nature* **2003**, *425*, 145.
(22) Piirma, I. *Emulsion Polymerization*; Academic: New York, 1982.
(23) Halperin, A.; Tirrell, M.; Lodge, T. P. *Adv. Polym. Sci.* **1992**, *100*, 31.
(24) See, for example: (a) Zhang, L.; Eisenberg, A. *Science* **1995**, *268*, 1728. (b) Ma, Y. H.; Cao, T.; Webber, S. E. *Macromolecules* **1998**, *31*, 1773. (c) Jenekhe, S. A.; Chen, X. L. *Science* **1998**, *279*, 1903. (d) Sommerdijk, N. A. J. M.; Holder, S. J.; Hirons, R. C.; Jones, R. G.; Nolte, R. J. M. *Macromolecules* **2000**, *33*, 8289. (e) Moffit, M.; Khougaz, K.; Eisenberg, A. *Acc. Chem. Res.* **1996**, *29*, 95.
(25) Wang, G.; Tong, X.; Zhao, Y. *Macromolecules* **2004**, *37*, 8911.
(26) Li, Y. B.; He, Y. N.; Tong, X. L.; Wang, X. G. *J. Am. Chem. Soc.* **2005**, *127*, 2402.
(27) Li, Y. B.; Deng, Y. H.; He, Y. N.; Tong, X. L.; Wang, X. G. *Langmuir* **2005**, *21*, 6567.

(28) Rau, H. *Photochemistry and Photophysics*; Rabek, J. F., Ed.; CRC Press: Boca Raton, FL, 1990; Vol. II., Chapter 4.
(29) Wu, L.; Tuo, X.; Cheng, H.; Chen, Z.; Wang, X. *Macromolecules* **2001**, *34*, 8005.
(30) Zhang, L.; Eisenberg, A.*J. Am. Chem. Soc.* **1996**, *118*, 3168.
(31) Terreau, O.; Luo, L. B.; Eisenberg, *Langmuir* **2003**, *19*, 5601.
(32) Zhang, L.; Shen, H.; Eisenberg, A. *Macromolecules* **1997**, *30*, 1001.
(33) Burchard, W. *Makcromol. Chem. Macromol. Symp.* **1988**, *18*, 1.
(34) Antonietti, M.; Heinz, S.; Schmidt, M.; Rosenauer, C. *Macromolecules* **1994**, *27*, 3276.
(35) Kumar, G. S.; Nechers, D. C.*Chem. Rev.* **1989**, *89*, 1915.
(36) Zollinger, H. *Azo and Diazo Chemistry*; Interscience Publisher Inc.: New York, 1961.
(37) (a) Schultz, T.; Quenneville, J.; Levine, B.; Toniolo, A.; Martinez, T. J.; Lochbrunner, S.; Schmitt, M.; Shaffer, J. P.; Zgierski, M. Z.; Stolow, A. *J. Am. Chem. Soc.* **2003**, *125*, 8098. (b) Satzger, H.; Root, C.; Braun, M. *J. Phys. Chem. A* **2004**, *108*, 6265.
(38) Sin, S. L.; Gan, L. H.; Hu, X.; Tam, K. C.; Gan, Y. Y. *Macromolecules* **2005**, *38*, 3943.
(39) Victor, J. G.; Torkelson, J. M. *Macromolecules* **1987**, *20*, 2241.
(40) (a) Price, C. *Pure Appl. Chem.* **1983**, *55*, 1563. (b) Price, C.; Chan, E. K. M.; Mobbs, R. H.; Strubbersfield, R. B. *Eur. Polym. J.* **1985**, *21*, 355. (c) Price, C.; Chan, E. K. M.; Strubbersfield, R. B. *Eur. Polym. J.* **1987**, *23*, 649.

MA052272Y